

# Report on alignment/tuning/diagnostics at ATF and plans for JLC

Junji Urakawa and Hitoshi Hayano

High Energy Accelerator Research Organization(KEK), 1-1 Oho, Tsukuba-shi, Ibaraki, Japan

## Abstract

This report describes the results of the magnet alignment, beam tuning and diagnostics of the ATF at KEK and the future plan of the instrumentation for JLC. The purpose of the ATF is to generate beams with very small transverse and longitudinal emittances as required for future linear colliders.

## 1 OUTLINE OF ATF AT KEK

The Accelerator Test Facility (ATF) at KEK consists of three major parts: an S-band injector linac, a damping ring, and a beam diagnostic section(EXT) (see Fig. 1) [1]. Each part directly contributes to the development of technologies relevant to high luminosity linear colliders. The ATF has been designed to investigate the feasibility of the LC operation scheme and to develop beam-control techniques for the LC [2, 3, 4]. The multibunch scheme is essential to boost the rf-to-beam transfer power efficiency in the accelerator. The ATF generates, accelerates, damps, and extracts a train of 20 bunches with  $1 \times 10^{10}$  electrons/bunch and 2.8ns spacing. A newly developed damped cavity suppresses the coupled-bunch instabilities in the damping ring. A new simultaneous injection-extraction system for the damping ring will solve the problem of transient beam loading due to multi-train operation in the damping ring.

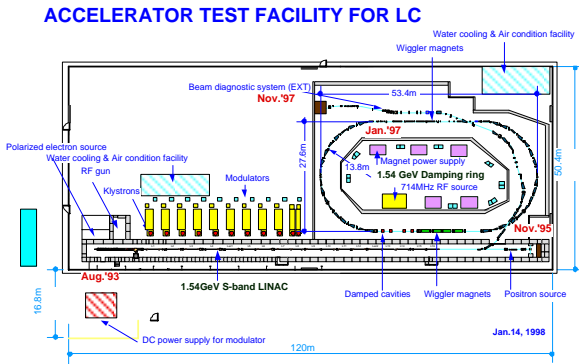


Figure 1: The Accelerator Test Facility (ATF) at KEK.

The goal is to achieve a normalized emittance of  $5 \mu\text{m}$  horizontal and  $0.02 \mu\text{m}$  vertical and a 0.08% energy spread for the multibunch beam. The small emittance from the damping ring has been achieved by special design of a strong focusing lattice with precise alignment of components and beam orbit control. The nonlinear behavior of

the beam has to be well understood to provide enough dynamic aperture under such strong focusing conditions. The layout of the EXT for precise beam diagnostics is shown in Figure 2.

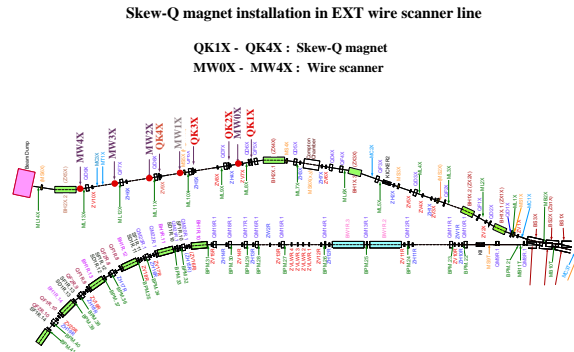


Figure 2: The layout of the extraction line.

## 2 EMITTANCE MEASUREMENTS AT THE EXT

Intensive studies on the vertical emittance with the wire scanners in the EXT have been ongoing since March(2000) [5]. An important observation we made during this time is that there appears to be a source of x-y cross plane coupling somewhere between the extraction point of the damping ring (DR) and the wire scanner region in the EXT. The measured vertical emittance is approximately  $(1.1 \pm 0.1) \times 10^{-11} \text{m}$  for the beam intensity of  $(2.0 \pm 0.2) \times 10^9$  electrons per bunch. This represents the best result so far obtained at the EXT in a single-bunch mode operation. The emittance is found to grow to  $(2.2 \pm 0.1) \times 10^{-11} \text{m}$  at the beam intensity of  $(8.0 \pm 0.3) \times 10^9$  electrons per bunch, however. This could be due to effects of the intra-beam scattering, which according to a simulation can lead to an emittance growth of  $\sim 50\%$  at this bunch intensity. More careful theoretical and experimental studies are needed to fully understand the situation. In these measurements, the x-y beam profile showed a tilting of a few degrees, as observed by using 10 degree wires. The quoted vertical emittance in these plots might be further reduced by re-optimizing the setting of skew magnets. Obviously, repeated measurements and careful studies are needed, and the results shown here should be considered preliminary. It appears that the following points play an important role.

1. Tuning with skew knobs in the arc sections of the DR for reducing the betatron coupling in the ring.
2. Careful corrections for residual dispersion in the EXT.
3. Additional cross-plane coupling correction using a skew quadrupole magnet in the EXT, upstream of the wire scanners.

### 3 MAGNET ALIGNMENT IN DAMPING RING

The damping ring uses many active girders for the beam based alignment. This system is not yet completed. One active girder in the arc section supports one combined bending magnet, two quads and two sextupoles. About 300 magnets for ATF damping ring were aligned within the accuracy of  $\pm 100\mu\text{m}$  (peak-to-peak) until now. Since main magnets on the active girder in the arc section are set within the accuracy of  $37\mu\text{m}$  (r.m.s.), we can align them precisely using beam based alignment and movers. The scattered plot on setting error of transverse position and longitudinal setting error are shown in Figure 3.

Also, the ring circumference has been measured. Figure 4 shows difference between measured circumference and design one of the damping ring. We have changed rf frequency in the range of  $20\text{kHz}$  to  $20\text{kHz}$  because of keeping the centered beam orbit in the arc-sections. This corresponds the circumference change of the ring in the range of  $-3\text{mm}$  to  $3\text{mm}$ . The circumference expands until Aug. by 6mm and shrinks to measured values on Jan. when we started operation of the ring 1997. Rate of concrete expansion is about  $10^{-5}/\text{degree}$ . Thermal expansion is main source of this problem because calculated values is consistent with measurements.

### 4 BEAM TUNING AND DIAGNOSTICS IN DAMPING RING

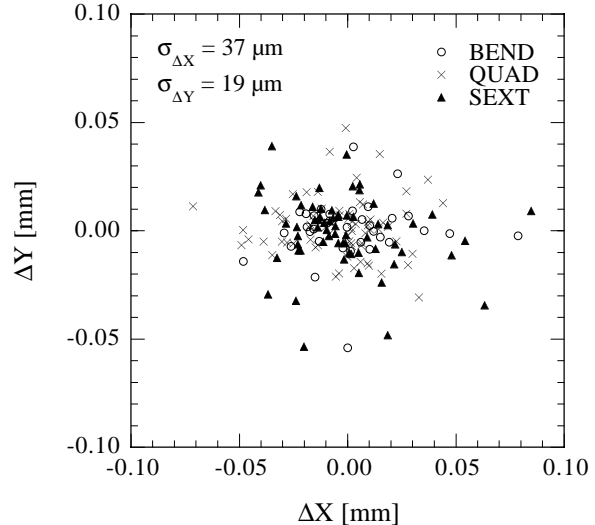
#### 4.1 COD and Dispersion

The program SAD is used in orbit and dispersion corrections, for calculating new setting of the steering magnets. The COD correction in DR was satisfactory, but the results were 2mm (peak to peak) horizontally with 1 mm expected from simulations and 1 mm vertically. The reason may be misalignment of magnets, errors in the optics model (especially non-linearity) and error of BPMs. The dispersion in the DR is measured as difference of orbits with different RF frequencies. The dispersion correction in the ring worked and typical r.m.s. of the vertical dispersion after the correction was about 5 mm which is close to our target.

#### 4.2 X-Y Coupling

To correct  $x$ - $y$  coupling, trim coils of the all sextupole magnets are connected to produce skew quadrupole field. A global correction of the coupling is essential to achieve the smaller emittance. We tried a global coupling correction minimizing vertical COD response to horizontal steering.

Assembly Result of Magnets on Mover Table Transverse Direction



Assembly Result of Magnets on Mover Table Longitudinal Direction

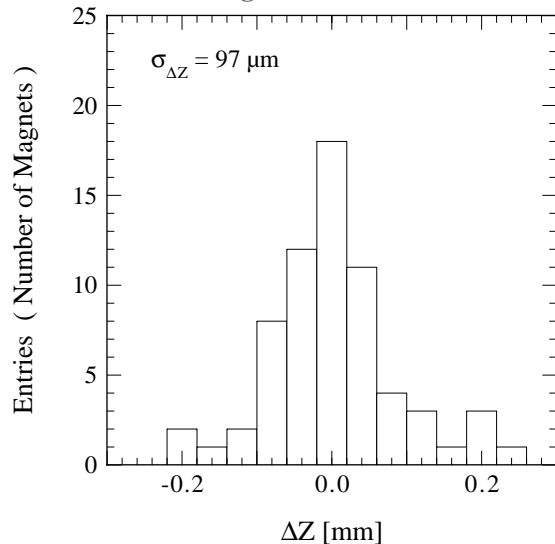


Figure 3: Scattered plot on transverse setting error and longitudinal setting error which were measured on magnets of the ATF 14 active girders using a 3D mobile tracking system.

The orbit coupling was clearly reduced and some reduction of the vertical emittance was observed after the correction. We also tried a coupling correction by 4 dedicated skew quadrupoles and achieved some reduction in the vertical beam size at the SR source point.

Local orbit bumps were also used for low vertical emittance. Setting many bumps one-by-one the vertical beam size was monitored using SR-interferometer. Probably, the resolution (or stability) of the monitor was not enough for this tuning technique.

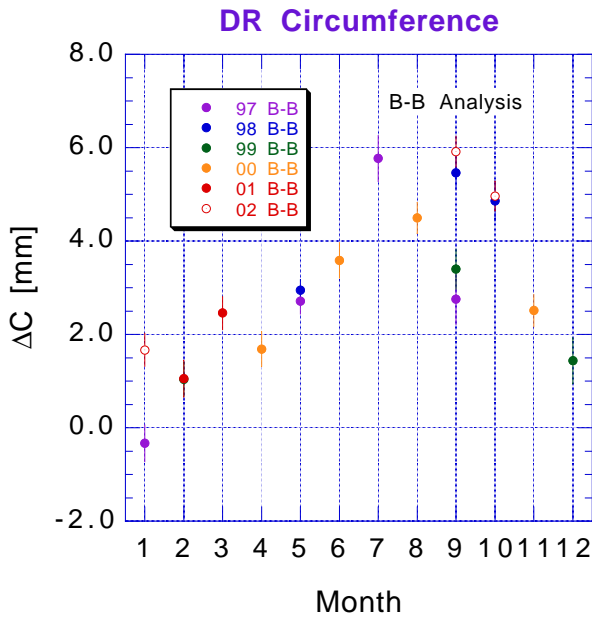


Figure 4: Change of Damping Ring Circumference, Horizontal axis indicates month on which the circumference was measured. Vertical axis is the difference between measured values and design one.

### 4.3 Optics Diagnostics

The error in the original estimation of the quadrupole field of each type of the quadrupole magnets was calculated from the response to beam-orbit change and the model was corrected. The errors of some types of magnets were as large as 2%. We measured the  $R_{12}$  single-pass response matrix of each BPM to excitations of the different dipole correctors, with sextupole magnets turned off. From these data we calculated typical quadrupole field-strength errors of about 1% and upgraded the optics model so as to account for these errors, which arise from an interference effect between adjacent magnets. The magnetic-field difference between the upgraded model and new beam-based measurements are less than 0.01%.

### 4.4 Beam-Based Alignment

Some pilot experiments of beam based alignment were done, changing strength of quadrupole one by one and measuring the beam orbit. The results were consistent with the conventional alignment measurement but the accuracy is not better than the conventional measurement. Simulations show that we need a better BPM resolution.

### 4.5 Future Plans

Our goal is to confirm the stable operation with 3 trains in the DR towards the end of JFY2003. Each train should consist of 20 bunches with bunch spacing of 2.8 nsec. There are many study items on the multi-bunch beam physics. For

example, transient beam loading, multi-bunch instabilities, fast ion instability and emittance blow-up issues due to the multi-bunch beam which should be overcome.

The following development studies are under way in collaboration with Japanese universities and foreign accelerator physicists. Future plans address the immediate goals of understanding the minimum achievable single bunch emittance and obtaining stable operation with  $3 \times 20$  bunch trains. A program of theoretical and experimental studies has been planned that is focused on understanding the correction and optimization procedures, the stability of the ring component alignment, intra-beam scattering emittance growth and the multi-bunch beam dynamics mentioned before.

## 5 PLANS FOR INSTRUMENTATION OF JLC

### 5.1 Beam Position Monitors

The most important instrumentation for the beam control is beam position monitors (BPM), which measure the transverse positions of the beam centroid. The capability requirements for the BPM at JLC include: a single pass measurement, an average position measurement for a multi-bunch beam, a 150 Hz data acquisition speed, high resolution, and high accuracy. High-precision orbit control of the order of several  $\mu\text{m}$  is required for the beamlines and accelerators downstream of the main damping rings. The RF BPM technology is applied for these high resolution, high accuracy BPMs. In other areas, the precision requirement is relaxed to several  $10\mu\text{m}$ . Strip line BPMs and the button BPMs are used for them.

**Stripline BPM for the Linac upstream of DR and the Compressor Arc** This BPM is used in Linacs and the beam transport lines upstream of the main damping rings. It is also used in the arc sections of the bunch compressors (BC2 arcs). This BPM has  $50 \Omega$  striplines (40 mm long) with one shorted end. In upstream linacs a BPM is directly mounted on a quadrupole magnet, as shown in Fig. 5. In the BC2 arc sections, where a relatively large aperture is necessary, the BPMs are rolled by  $45^\circ$  and placed on a mount.

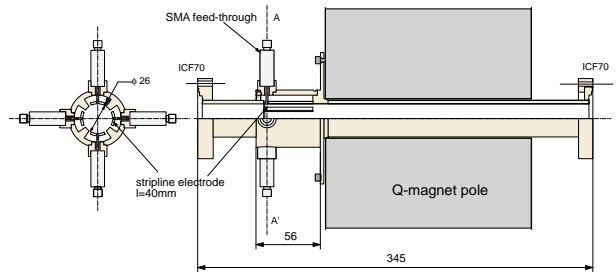


Figure 5: Stripline BPM.

The expected resolution for beam position measurement is  $1\mu\text{m}$ . The deviation in the electrical center of a BPM

from its quadrupole center is controlled to within  $50\mu\text{m}$ . This includes the effects of the calibration accuracy of the mechanical and electrical offsets, the stability of the electrode position, as well as the stability of the signal processing electronics. A calibration method with a singing wire is applied after each BPM is installed on its quadrupole magnet. The electronics will be equipped with a self-calibration system, too. The read-out system employs a base line clipping circuit and a charge ADC for good performance and low cost.

**Button BPM for DR and Pre-DR** In the main damping rings (DRs) and the positron pre-damping ring (pre-DR), button type electrode BPMs are used, since they can fit within a small space and offer a relatively low coupling impedance to the beam. Fig. 6 shows their schematic design. This design is very similar to that of the BPMs for ATF. However, the diameter of the electrodes has been chosen to be 8 mm, smaller than the 12 mm of the ATF BPMs, to reduce the heating due to SR light.

The DR BPMs are welded onto the vacuum chamber. Calibrations of the BPM offset and position mapping are done, after the vacuum chamber assembly is completed, by using a long rigid antenna. For signal processing, the same electronics system as that for the stripline BPMs will be used for the button BPMs. The resolution and accuracy of the button BPMs are expected to be comparable to that of the strip line BPMs:  $1\mu\text{m}$  for resolution and  $50\mu\text{m}$  for the absolute accuracy. However, the mechanical stability of the DR button BPMs is more difficult to maintain than for stripline BPMs at upstream linacs. This is because of the large heat load on the vacuum chamber and the BPM electrodes contacting the thin central conductor of the SMA feed through. Thus, to maintain accurate knowledge of the BPM centers, it is essential to rely on the beam based alignment (BBA) technique.

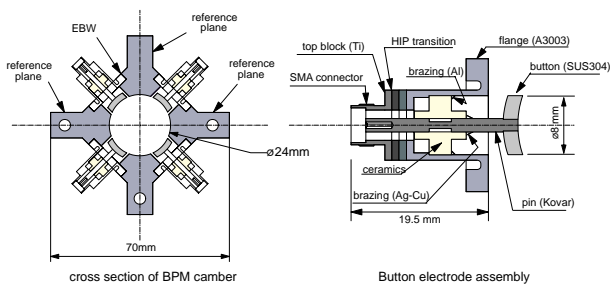


Figure 6: DR button BPM.

**RF BPM for Q-BPM at downstream of DR** For BPMs in the area downstream of the DRs, a mechanical stability of  $1\mu\text{m}$  or better in any time scale is required during operation. The RF BPMs based on a microwave cylindrical cavity have a much more rigid structure than other BPMs. Consequently, a superior long-term mechanical stability is expected, and the RF BPMs are considered

to be suited for deployment in this area. Their resolution is  $0.1\mu\text{m}$  over a measurement range of  $\pm 50\mu\text{m}$ . The absolute accuracy is  $10\mu\text{m}$ . Since the sensor cavity and its outer surface has a concentric, cylindrical shape, their centers can be determined within a few  $\mu\text{m}$ . The installation into the quadrupole magnet, as shown in Fig. 7, and the calibration of the BPM center to the magnetic center is done to an accuracy of  $10\mu\text{m}$ . The singing wire method determines the magnetic center, and an external coordinate machine correlates it to the BPM outer surface, which is the reference surface of the BPM.

Temperature control is essential for maintaining the mechanical stability. The BPM temperature is affected by the ambient temperature and heat from the quadrupole magnet. An electrical temperature controller with a  $\pm 0.1$  degree accuracy is installed in the BPM body. Drifts of the BPM offset due to common mode contaminations are suppressed by employing the slot magnetic coupling and the external suppressor circuit using two port combiner. The frequency of the difference mode in the sensor cavity is chosen to be 6.5 GHz, since it has no relation to any accelerator frequency. This allows one to avoid interference into the circuit. The detection circuit consists of a synchronous phase detector with the reference cavity pickup, a pulse stretching amplifier, a diode amplitude detector, a pulse amplifier and a 16 bit track-hold ADC.

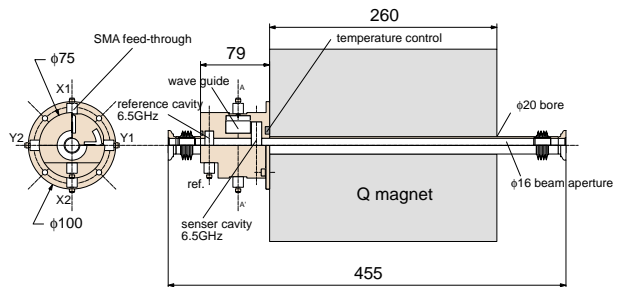


Figure 7: RF BPM at a Q magnet.

**Acc. HOM BPM for Main Linac structure** The RF signals of the difference mode from 4 higher order mode port are equivalent to the RF BPM signal, except for the reference signal. They are a measure of the beam off center from the structure center. These signals should be minimized by activating the structure mover when the beam is well aligned to the center of the quadrupole magnets. The detection circuit is the same as the RF BPM. The reference signal for the synchronous phase detector is taken from the common mode signal coming out from the same port. The difference mode and the common mode signal are coupled out to each port of the combiner. The resolution of the structure position is  $0.1\mu\text{m}$ . The circuit should be protected from the high power signal resulting from a breakdown in the structure.

## 5.2 Beam Size Monitors

**Carbon-wire scanner at upstream of DR** The use of destructive beam size monitor should be avoided in the accelerator, because of the high power beam and the high radiation yield. A carbon wire scanner is a reliable and precise beam size monitor with a small disturbance. The beam power is sufficiently high to break a tungsten wire; a carbon wire of  $7\ \mu\text{m}$  diameter can withstand it. Monitors are installed in several places, with 4 scanners set upstream of the damping ring. The scanner chamber and its mechanics are the same as the ATF wire scanner. They have a  $0.5\ \mu\text{m}$  mover resolution and a  $0.5\ \mu\text{m}$  wire position read back resolution. The carbon wires are stretched as shown in Fig. 8. A gamma-ray detector placed downstream of the scanner detects gamma rays from beam-wire interaction.

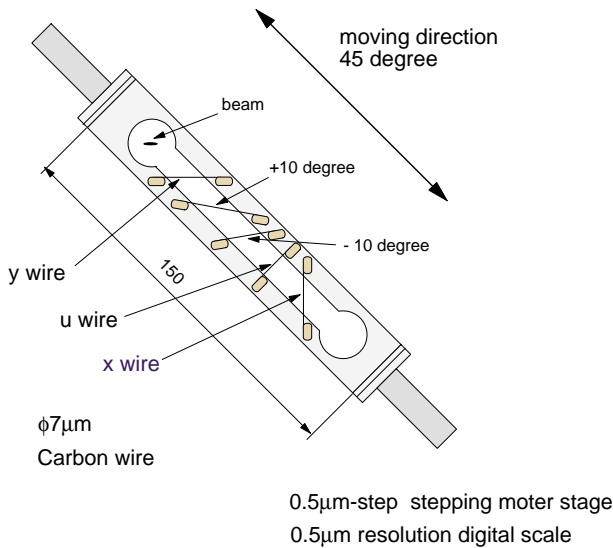


Figure 8: Carbon wire mount in the wire scanner.

**Laser-wire scanner downstream of DR** Downstream of the main damping ring, the beam size becomes very small (around  $100 \times 10\ \mu\text{m}$ ), while the bunch charge remains the same. Since the carbon wire cannot withstand the condition in such a high density beam, a laser wire scanner is used there as a non-break wire. The laser wire is produced in the optical cavity, while keeping in resonance by a piezo-mirror control. A pulsed laser beam is supplied through an optical fiber into the cavity. For a sufficient gamma-ray yield during scanning and to avoid fiber damage, the laser peak power is 300 W and a  $100\ \mu\text{m}$  pulse length is used inside the lead shield housing on the floor. The laser wire chamber consists of  $x$  and  $y$  laser wires and RF BPM on both sides, as shown in Fig. 9. The beam chamber with a  $\phi\ 16\text{mm}$  inner diameter has a pair of  $\phi\ 3\text{mm}$  holes for the laser. The wire is moved together with the chamber within the bellows stretching limit. The mover resolution is  $0.5\ \mu\text{m}$ . Since the yield of the generated gamma-ray is much less than the carbon wire, the scanning

time will be much longer, like 1 or 2 minutes for one profile. The gamma-ray detector is the same as that of the carbon wires [6].

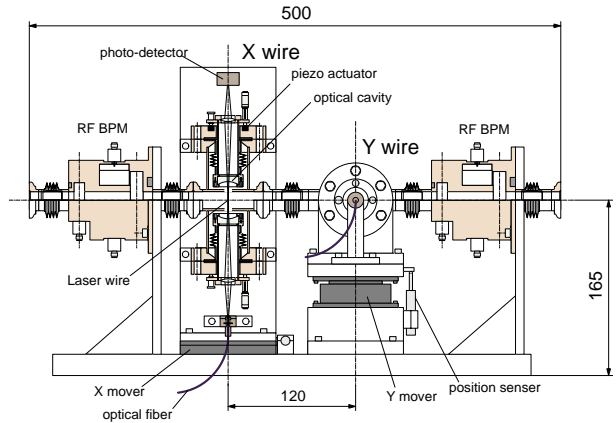


Figure 9: Laser wire scanner.

### Laser interference monitor at I.P. for startup tuning

Direct monitoring of the beam size of the interaction point is only required during the machine startup time. After the detector facility rolls in, the colliding beam size is monitored by other methods, such as the beam-beam deflection technique. The laser interference monitor uses the interaction of the beam with laser interference fringe, and observes the gamma-ray modulation by scanning the beam. This monitor was already demonstrated while detecting a  $60\ \text{nm}$  beam size in the FFTB experiment.

### Bunch length monitor at bunch compressor

For the tuning and monitoring of the bunch compressor, a bunch length monitor with a  $10\ \mu\text{m}$  (30fs) resolution is required. The spectrum reconstruction monitor in the infra-red region is used for the  $100\ \mu\text{m}$  bunch length measurement. Optical diffraction radiation (ODR) is the source of infra-red beam radiation, since there is no gamma-ray radiation which gives damages to the accelerator.

### Acknowledgements

The authors would like to thank Professors H.Sugawara, Y.Kimura, S.Yamada, S.Iwata, Y.Kamiya, K.Takata, S.Kurokawa, and A.Enomoto for their encouragement. All members of KEK-ATF group and international collaborators for this research program are acknowledged. We also thank Professor E.Paterson and Professor D.Burke of SLAC and K.Hubner of CERN for supporting the ATF project as an international collaboration.

## 6 REFERENCES

- [1] Edited by F.Hinode, et al., KEK Internal 95-4, June 1995.
- [2] J.Urakawa, KEK/ATF Damping Ring, PAC97, pp.444-448, Vancouver, May 1997.
- [3] Edited by H.Hayano et al., KEK Internal 2000-6 A (2000).

- [4] J.Urakawa et al., presented at 17th International Conference on High-Energy Accelerators (HEACC98), Dubna, Russia, 7-12 Sep. 1998. KEK Preprint 98-154.
- [5] J.Urakawa, H.Hayano and M.Ross, Proc. of this conference.
- [6] Y.Honda et al., Proc. of this conference.